

## EXPERIMENTAL RESULTS ON CRACK INVERSION

L. Ahlberg and B. R. Tittmann

Rockwell International Science Center  
Thousand Oaks, CA 91360

A. N. Norris and J. D. Achenbach

The Technological Institute  
Northwestern University  
Evanston, IL 60201

### ABSTRACT

The work reported here is part of a program on flaw detection in turbine rotor components. The goal is to image or map non-surface breaking fatigue cracks near the bore hole surface of an aircraft engine disk with the aid of ultrasonic inversion techniques. Presented are results of inversion of both pitch-catch and pulse-echo data with the inversion technique discussed in detail in the companion paper [1].

### INTRODUCTION

The inversion technique is based on the diffraction of elastic waves by the crack-edge and employs Achenbach's elastodynamic ray theory and the geometrical theory of diffraction [2]-[4]. Two analytical methods were developed for mapping the edge of a crack; the first, henceforth identified as  $A_1$ , maps flash points on the crack edge by a process of triangulation with the source and receiver as given vertices of the triangle. By the use of arrival times at neighboring positions of the source and/or the receivers, the directions of signal propagation, which determine the triangle, can be computed. This inverse mapping is global in the sense that no a-priori knowledge of the location of the crack edge is necessary. The second method, henceforth identified as  $A_2$ , is a local edge mapping which determines planes relative to a known point close to the

crack edge. Each plane contains a flash point. The envelope of the planes map an approximation to the crack edge. This method was found to give much better accuracy than the global triangulation method. An additional useful feature of the local mapping technique is that it allows for an iteration procedure whereby the result of a computation suggests an improved choice of the base point which in the subsequent iteration yields a better approximation to the crack edge.

#### EXPERIMENTAL APPROACH

The experiments were carried out on a spherical specimen (trailer hitch) which contains an elliptical (yttria) crack at its center. The material of the sphere is Ti-alloy. Similar experiments have been discussed in Ref. [5]. Since the material is somewhat anisotropic, the velocity of longitudinal waves depends on the polar angle. Representative values are given in Table 1.

Table 1  
Dependence of Longitudinal Wave Speed on Polar Angle

Polar Angle $\phi$ (degrees)	Sample #37 ( $c_L$ mm/ $\mu$ sec)	Sample #39 ( $c_L$ mm/ $\mu$ sec)
55.5	6.193	6.175
73.5	6.219	6.203
90	6.232	6.215

The radius of the sphere is 27.94 mm. The yttria crack is almost elliptical with major and minor axes of 2.57 and 1.41 mm, respectively. The geometrical configuration is shown in Fig. 1. The crack is located in the xy-plane, with its center at the center of the sphere.

For each specific set of data the position of the receiver transducer was at a fixed value of the polar angle  $\phi$ , but the azimuthal angle  $\psi$  was varied incrementally. In order to obtain accurate measurements from the sample, a precision goniometer was constructed. This device allows fine control of the position of the center of the spherical sample and provides a good contact of the transducer with the specimen. The experiments were made in pitch-catch and pulse-echo using 5 and 15 MHz broadband longitudinal transducers with the transmitting

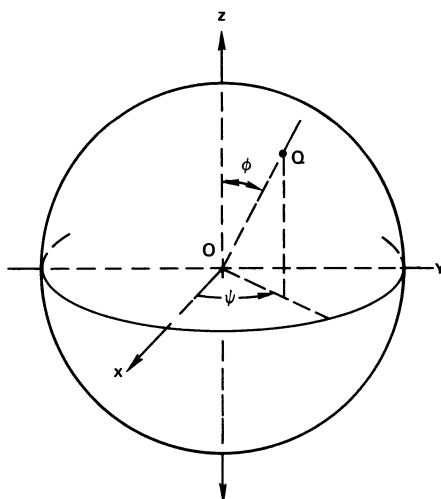


Fig. 1 Geometry of Ti-alloy sphere with source point S. The elliptical crack is in the xy-plane.

transducer hard bonded to the sample. The bonding material was Devcon 5 minute epoxy.

The arrival times of the edge-diffracted signal were estimated by visual inspection of the waveforms plotted versus time. Figure 2 shows an example by presenting the set of time-domain waveforms for one of the data sets.

The arrival times of the edge-diffracted signal are estimated by visual inspection of the waveforms plotted versus time (Fig. 3). The same point of the waveform is consistently selected as defining the arrival time. Any random errors are effectively removed by regularizing the data, i.e., by plotting the data versus time and fitting a least-square-fit curve through the data points.

#### INVERSION OF PITCH-CATCH DATA

Pitch-catch data were obtained in the form of travel times between the transmitter (TX) and receiver (RC) for the following configurations:

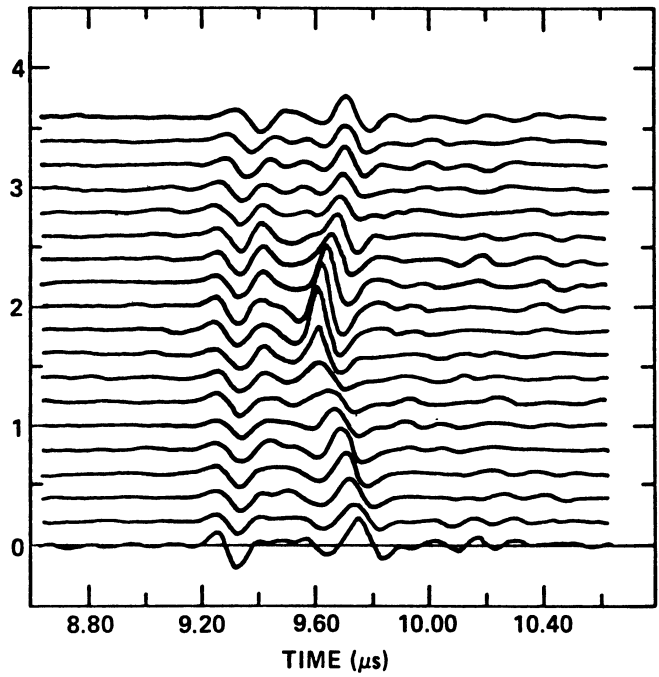


Fig. 2 Waterfall plot of 19 waveforms in the time domain for the transmitter at  $\phi = 10$ ,  $\phi = 0$  and the receiver at  $\phi = 65$ ,  $\phi = j \times 10$  ( $j = 0$ , integer, 1 - 18).

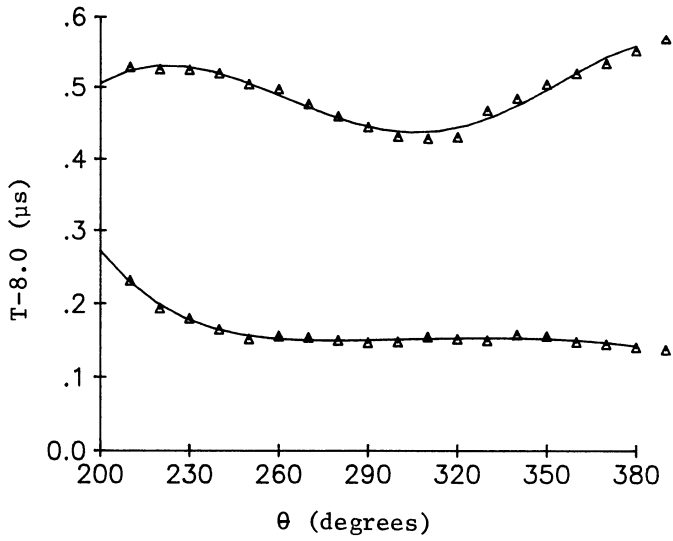


Fig. 3 Experimental data ( $\Delta$ ) with least square fit curve.

- I. TX  $\phi = 20^\circ, \theta = 0^\circ$   
RC  $\phi = 112^\circ, \theta = j \times 10^\circ (j = 1 \rightarrow 18)$
- II. TX  $\phi = 10^\circ, \theta = 0^\circ$   
RC  $\phi = 65^\circ, \theta = j \times 10^\circ (j = 3 \rightarrow 21)$
- III. TX  $\phi = 10^\circ, \theta = 0^\circ$   
RC  $\phi = 65^\circ, \theta = j \times 10^\circ (j = 15 \rightarrow 3)$
- IV. TX  $\phi = 20^\circ, \theta = 0^\circ$   
RC  $\phi = 65^\circ, \theta = j \times 10^\circ (j = 17 \rightarrow 3)$

Each of the four sets of data corresponds to one of the two sets required for inversion. Without any a priori knowledge of the work location or orientation, we must use two sets simultaneously if we are to find the crack. Figure 4 shows the result of applying the general method to data sets I and II. Both algorithms  $A_1$  and  $A_2$  have been used and Fig. 4 shows the final results after iteration. The algorithm  $A_2$  produces more flash points than  $A_1$  although the general shape defined by each is similar. We note from Fig. 4 that the projection of the results on the x-y plane corresponds to the correct shape of the crack which is known to be oriented at  $45^\circ$  to the x-axis. However, not all the computed points lie in the correct plane.

We note that as in Ref. [5] it was necessary to subtract a uniform time from the experimental data. The effect of not doing so is to alter radically the geometrical shape of the computed points. For a further discussion on this point see Ref. [5]. For the present data, it was found that the raw data was uniformly about 0.4 microseconds too large. This may be attributable to constant system delays and/or mechanical delays due to the finite size of the transducers, the bonding, etc.

Greater accuracy in the crack mapping is obtained if we assume the plane of the crack. Flash points may be determined by simply intersecting adjacent planes from the data sets and then intersecting these lines with the known crack plane. The results of this procedure are illustrated in Fig. 5.

#### INVERSION OF PULSE-ECHO DATA

The pulse-echo measurements were made at a constant polar angle of  $55^\circ$  while the azimuthal angle was varied between  $200^\circ$  and  $380^\circ$  in  $10^\circ$  increments. These data are insufficient for the application of the general method described in [4]. We have only one of the two sets of data required. However, we can proceed with the inversion if we assume the plane of the

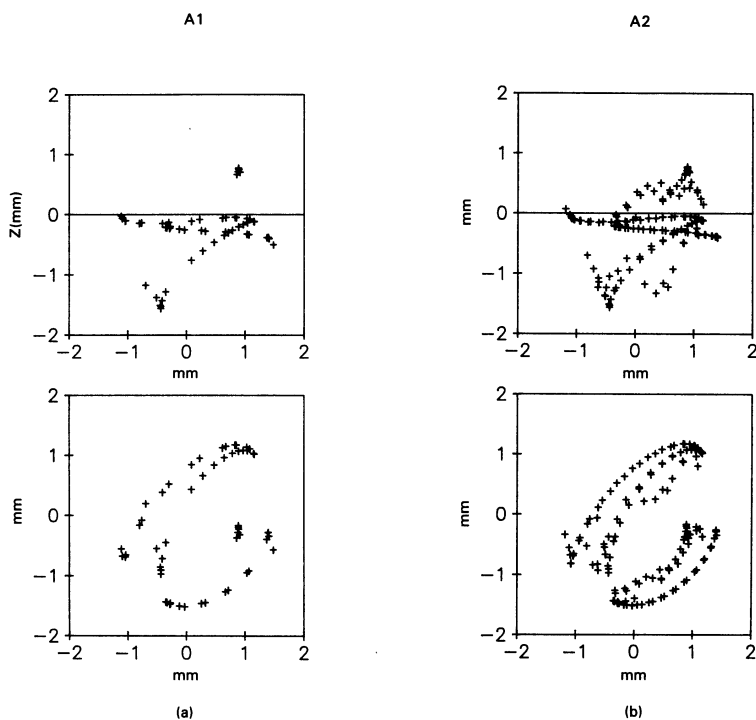


Fig. 4 Inversion results for data sets I and II (Top: sideview of crack plane. Bottom: projection of results onto x-y plane). (a) inversion with method A<sub>1</sub>; (b) inversion with method A<sub>2</sub>.

crack. The flash points are then found in the same fashion as they were for Fig. 5.

The results for the pulse-echo data are shown in Fig. 6. As with all the previous data, it was found necessary to decrease the experimentally measured travel times by a constant

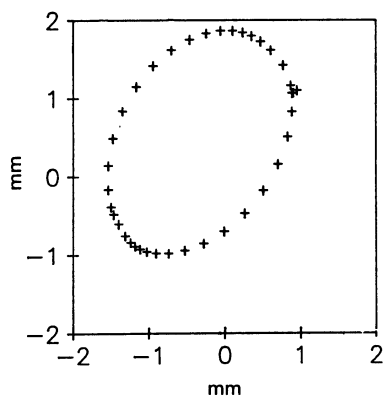


Fig. 5 Inversion results for data sets I and II assuming the plane of the crack.

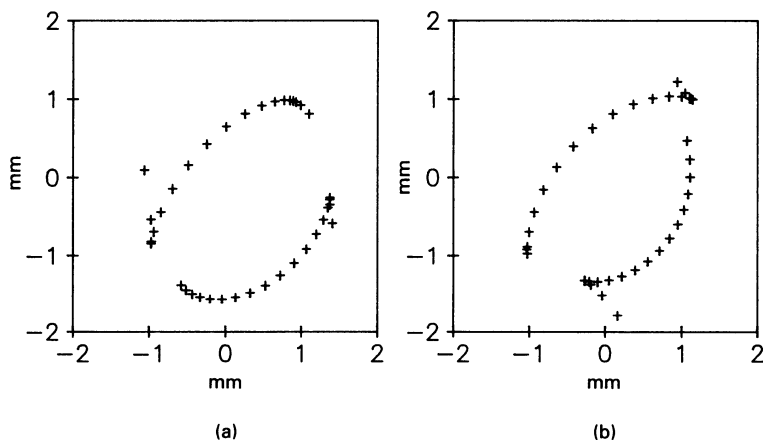


Fig. 6 Two trial inversions for pulse-echo data assuming the plane of the crack.

amount. For the pulse-echo data, this amount was found by trial and error to be  $0.3 \mu\text{sec}$ . The results when this uniform correction is not included are shown in Fig. 7a. Other values of the uniform correction give the results of Figs. 7b and c. An

overlarge decrease of  $0.5 \mu\text{sec}$  was taken in Fig. 7b while in Fig. 7c the decrease is  $0.25 \mu\text{sec}$ . We note that an incorrect uniform time tends to involute the crack edges. In Ref. [5], we have discussed how a uniform error in the travel time effects the general mapping method. It was shown using synthetic data that the error resulted in a mapped crack which was shifted and rotated in space. The general shape of the mapped crack did not

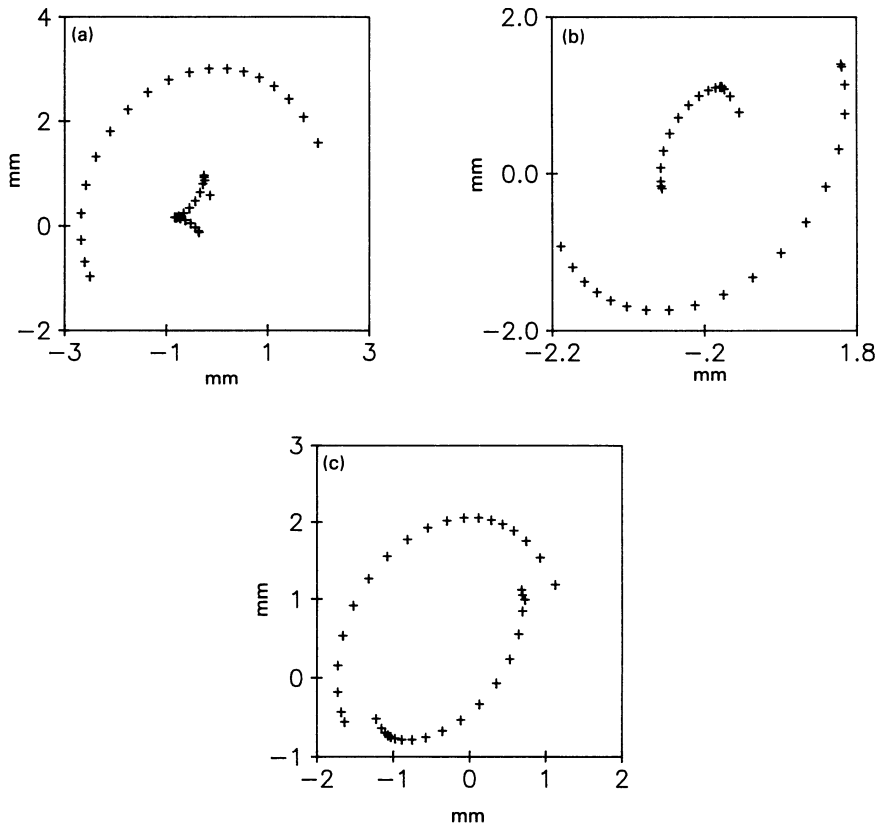


Fig. 7 Three trial inversions for several different uniform, constant travel-time corrections  $\Delta$ . (a)  $\Delta = 0 \mu\text{sec}$ , no corrections (b)  $\Delta = 0.5 \mu\text{sec}$  (c)  $\Delta = 0.25 \mu\text{sec}$ .

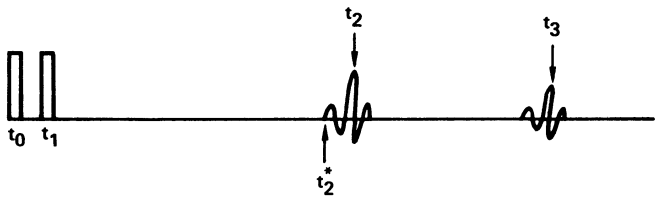


vary much from the correct shape as long as the uniform error remained small. In Fig. 7 we are not using the general mapping method but are a priori assuming the plane of the crack. Therefore, it is important to note the distinction between the present results and those of Ref. [5-8].

DETERMINATION OF START TIME OF ACOUSTIC PULSE

Calibration measurements were carried out to account at least in part, for the uniform adjustment in waveform arrival times necessary for the inversion. Possible sources for errors were thought to be due to delays in system trigger times, delay in coaxial cables, amplifier delays and transducer characteristics. With the help of Ti-alloy samples, including a trailer-hitch without a defect in its center, a series of pitch-catch experiments were set up to transmit directly from source to receiver. The first and second echoes were recorded and the time difference measured. This number was subtracted from the first part of the first echo waveform to calculate the time when the acoustic signal left the transducer. This time was found to be about 0.2  $\mu$ sec later than the system trigger time. The calibration results are summarized in Table 2 and account in part for the necessary uniform adjustments in travel times discussed in Section 4.

Table 2  
Determination of Start Time of Acoustic Pulse



TRANSDUCER	DIAM (mm)	$t_3 - t_2$ $\mu$ s	$t_2^*$ $\mu$ s	$t_1$ $\mu$ s
SAMPLE A Ti 6-4				
5 MHz, SHEAR	6.35	21.80	22.00	0.200
5 MHz, LONG	12.7	9.27	9.45	0.180
15 MHz, LONG	6.35	9.26	9.45	0.190
SAMPLE B Ti 6-4				
15 MHz, LONG	6.35	11.72	11.91	0.190

## ACKNOWLEDGEMENT

This work was sponsored by the Center for Advanced Nondestructive Evaluation, operated by the Ames Laboratory, USDOE, for the Defense Advanced Research Projects Agency and the Air Force Wright Patterson Aeronautical Laboratories/Materials Laboratory under Contract No. W-7405-ENG-82 with Iowa State University.

## REFERENCES

1. A.N. Norris, J.D. Achenbach, L.A. Ahlberg and B.R. Tittmann, "Further Results for Crack-Edge Mappings by Ray Methods," this volume.
2. J.D. Achenbach and A.N. Norris, "Crack Characterization by the Combined Use of time-Domain and Frequency-Domain Scattering Data," 1981 AF/DARPA Review of Quantitative NDE, Plenum Publishing Corp.
3. J.D. Achenbach, A.N. Norris and K. Viswanathan, "Mapping of Crack Edges by Seismic Methods," Bull. Seism. Soc. Am. 72, pp. 779-792 (1982).
4. A.N. Norris and J.D. Achenbach, "Mapping of a Crack Edge by Ultrasonic Methods," J. Acoust. Soc. Am. 72, pp. 164-272 (1982).
5. J.D. Achenbach, A.N. Norris, L. Ahlberg and B.R. Tittmann, "Crack Mapping by Ray Methods," 1982 Review of Progress in Quantitative NDE, Plenum Publishing Co.
6. A.N. Norris, "Inverse Ray Tracing in Elastic Solids With Unknown Anisotropy," J. Acoust. Soc. Am. 73, pp. 421-426 (1983).
7. A.N. Norris, "Inverse Ray Tracing in Anisotropic Elastic Solids," 1982 Review of Progress in Quantitative NDE, Plenum Publishing Co.
8. J.D. Achenbach, A.K. Gautesen and H. McMaken, Ray Methods for Waves in Elastic Solids, Pitman, Boston-London-Melbourne, 1983.

## DISCUSSION

M.J. Buckley (Rockwell International Science Center): What was the defect size?

B.R. Tittmann: It was a 300-micron crack, fatigue crack.